

## Crystal and Molecular Structure of Bis(difluorophosphino)amine at $-110^{\circ}\text{C}$

By Michael J. Barrow,\* E. A. V. Ebsworth, Marjorie M. Harding, and Stephen G. D. Henderson,  
Chemistry Department, Edinburgh University, West Mains Road, Edinburgh EH9 3JJ

At  $-110^{\circ}\text{C}$ , crystals of  $\text{NH}(\text{PF}_2)_2$  are monoclinic, with  $a = 8.69$ ,  $b = 4.72$ ,  $c = 12.08$  Å,  $\beta = 98.3^{\circ}$  (0.3% estimated standard deviations assumed), space group  $P2_1/n$ , and  $Z = 4$ . The structure has been refined to  $R$  0.076 using 561 unique intensities obtained from microdensitometer measurements of the Weissenberg levels  $h0-4l$  taken with  $\text{Cu-K}\alpha$  radiation. The molecular structure approximates to  $C_{2v}$  symmetry with the following geometrical parameters:  $\langle\text{P-N}\rangle$  1.667(10),  $\langle\text{P-F}\rangle$  1.578(5) Å,  $\text{P-N-P}$  120.7(4),  $\langle\text{F-P-F}\rangle$  95.7(4) $^{\circ}$ . Although the hydrogen atom is not well located, the nitrogen co-ordination appears to be trigonal planar. There are weak intermolecular  $\text{H}\dots\text{F}$  interactions, and additionally one phosphorus atom is involved in  $\text{P}\dots\text{F}$  interactions. This phosphorus has three 'normal' bonds and two very long  $\text{P}\dots\text{F}$  contacts.

As part of a study of the structural chemistry of simple  $\text{PF}_2$  derivatives,<sup>1</sup> we have recently prepared and characterised  $\text{N}(\text{PF}_2)_3$ ,  $\text{NH}(\text{PF}_2)_2$ , and  $\text{PF}_2[\text{NH}(\text{SiH}_3)]$  and determined the structures of the first and third of these in the gas phase by electron diffraction.<sup>1-3</sup> In both compounds the co-ordination round the N atom appears to be planar. The i.r. spectrum of the silyl compound,<sup>3</sup> however, shows two bands of roughly equal intensity in the regions associated with both NH stretching and in-plane NH deformation. We interpreted this observation as showing that two conformers were present in the vapour, and the radial distribution curve obtained from the electron-diffraction study led us to conclude that the vapour consisted of a mixture of conformer A (86%), in which one P-F bond is roughly coplanar with the P-N and N-Si bonds, and conformer B (14%) in which the two P-F bonds are *gauche* to the N-H bond. When this compound is condensed on a cold plate the spectrum of the solid changes with time; after 600 s at 80 K only one band is present in the NH stretching and in the NH deformation regions, and the frequencies of the remaining bands correspond closely to the lower-frequency components of the pairs of bands in the spectrum of the vapour. The i.r. spectrum of  $\text{NH}(\text{PF}_2)_2$  in the vapour phase shows two NH stretching and two NH deformation bands,<sup>1</sup> and we have determined the structure of this compound in the crystal in order to discover more about the geometric features of these compounds and to explore the relationship between the i.r. spectra and the conformation adopted by the  $\text{PF}_2$  groups. This compound would be difficult to study by gas-phase electron diffraction because of the large number of overlapping peaks in the radial distribution curve.

### EXPERIMENTAL

*Crystal Data.*— $\text{HF}_4\text{NP}_2$ ,  $M = 153.0$ , Monoclinic,  $a = 8.69$ ,  $b = 4.72$ ,  $c = 12.08$  Å,  $\beta = 98.3^{\circ}$  (0.3% estimated standard deviations assumed),  $U = 490.3$  Å<sup>3</sup>,  $Z = 4$ ,  $D_c = 2.07$  g cm<sup>-3</sup>,  $\text{Cu-K}\alpha$  radiation (Ni filter),  $\lambda = 1.5418$  Å,  $\mu(\text{Cu-K}\alpha) = 82.6$  cm<sup>-1</sup>, space group  $P2_1/n$  ( $C_{2v}$ , no. 14) by systematic absences. Melting point  $-80^{\circ}\text{C}$ ; cell parameters and intensities measured at  $-110^{\circ}\text{C}$ .

A sample of bis(difluorophosphino)amine (a colourless liquid unstable in air) was sealed in a Lindemann glass capillary (0.5 mm internal diameter). Crystals were grown

'*in situ*' on a Nonius Weissenberg goniometer fitted with a Nonius nitrogen-gas stream attachment for low temperatures. The crystal used for data collection was roughly cylindrical (diameter 0.5 mm, length 0.8 mm). Intensities for 561 unique reflections were obtained from microdensitometer measurements of equi-inclination Weissenberg photographs taken for the levels  $h0-4l$ .† The intensities were corrected for Lorentz and polarisation effects, and for absorption using tabulated values of  $A^*$ .<sup>4</sup> The data were placed on an approximately uniform scale on the basis of exposure times.

The space group imposes no restriction on molecular symmetry for  $Z = 4$ . Co-ordinates for the two phosphorus atoms were obtained from a Patterson synthesis, and the remaining non-hydrogen atoms located from a Fourier synthesis. The structural parameters for non-hydrogen atoms were refined through several cycles of isotropic and anisotropic least-squares calculations. The hydrogen atom was located on a difference-Fourier synthesis as a peak of height  $0.7$  e Å<sup>-3</sup>; two peaks of similar height were also observed midway along the P-N bonds and other peaks and troughs (maximum  $\pm 0.8$  Å<sup>-3</sup>) were located close to heavy-atom sites. At this stage the data were scaled to the model, level-by-level, by a least-squares method. During the final refinement process all positional parameters, including those for hydrogen, were refined together with anisotropic vibration parameters for the non-hydrogen atoms, an isotropic temperature factor for the hydrogen atom, and a single overall scale factor. A weighting scheme was included,  $w^{-1} = 1 + 0.012(F_o - 9)^2$ , and the nine most intense reflections were excluded from the least-squares calculations on the grounds of extinction effects.

The final  $R$  factor was 0.076; a final difference-Fourier synthesis still showed peaks (0.5 and 0.8 e Å<sup>-3</sup>) in the centres of the P-N bonds, and peaks and troughs of up to  $\pm 0.8$  e Å<sup>-3</sup> close to heavy-atom sites. Scattering factors were taken from ref. 5 for P and N, from ref. 6 for H, and from ref. 7 for F. Allowance was made for both real and imaginary components of the anomalous scattering effects for P and F atoms.<sup>8</sup>

The final atomic parameters are given in Table 1, details of the intramolecular geometry derived therefrom in Table 2, and important intermolecular distances and angles in Table 3. Figure 1 shows the atomic labelling scheme and illustrates the intermolecular interactions, Figure 2 the approximate  $C_{2v}$  molecular symmetry. A list of observed

† Microdensitometry and initial data reduction were performed by the S.R.C. Microdensitometer Service, Daresbury Laboratory, Warrington WA4 4AD.

TABLE 1

Atomic parameters with estimated standard deviations in parentheses

Atom	$x/a$	$y/b$	$z/c$
P(1)	0.649 00(24)	0.417 5(6)	0.350 00(16)
P(2)	0.441 77(23)	0.644 1(5)	0.161 36(16)
F(1)	0.580 0(7)	0.252 2(14)	0.445 9(5)
F(2)	0.741 8(7)	0.642 1(16)	0.430 1(5)
F(3)	0.263 5(6)	0.568 3(14)	0.153 6(5)
F(4)	0.418 3(7)	0.974 0(14)	0.156 3(5)
N(1)	0.494 1(7)	0.607 5(16)	0.299 6(5)
H(1)	0.448(9)	0.677(19)	0.352(7)

TABLE 2

Molecular geometry

(a) Intramolecular distances (Å) with estimated standard deviations in parentheses

P(1)-N(1)	1.658(7)	P(2)-N(1)	1.675(7)
P(1)-F(1)	1.585(7)	P(2)-F(3)	1.580(5)
P(1)-F(2)	1.576(7)	P(2)-F(4)	1.570(7)
P(1) ... P(2)	2.898(3)	N(1)-H(1)	0.87(9)
H(1) ... F(1)	2.50(9)	H(1) ... F(3)	2.74(8)
H(1) ... F(2)	2.60(8)	H(1) ... F(4)	2.73(9)

(b) Intramolecular angles (°)

N(1)-P(1)-F(1)	99.3(4)	N(1)-P(2)-F(3)	99.2(3)
N(1)-P(1)-F(2)	100.2(4)	N(1)-P(2)-F(4)	99.0(3)
F(1)-P(1)-F(2)	95.5(3)	F(3)-P(2)-F(4)	95.8(3)
P(1)-N(1)-P(2)	120.7(4)	P(1)-N(1)-H(1)	112(5)
		P(2)-N(1)-H(1)	127(5)

(c) Torsion angles (°)

F(1)-P(1)-N(1)-P(2)	-136.9(5)
F(2)-P(1)-N(1)-P(2)	125.7(5)
F(1)-P(1) ... P(2)-F(3)	-6.0(4)
F(3)-P(2)-N(1)-P(1)	130.8(5)
F(4)-P(2)-N(1)-P(1)	-131.7(5)
F(2)-P(1) ... P(2)-F(4)	-6.8(4)

(d) Distances (Å) of atoms from the least-squares best plane defined by P(1), P(2), N(1), H(1)

P(1)	-0.001;	P(2)	-0.001;	N(1)	0.004;	H(1)	-0.002;
F(1)	-1.063;	F(2)	1.263;	F(3)	-1.176;	F(4)	1.161

TABLE 3

Intermolecular geometry

(a) Shortest contact distances (Å)

H(1) ... F(1 <sup>v</sup> )	2.505	F(1) ... F(1 <sup>v</sup> )	3.136
H(1) ... F(3 <sup>iii</sup> )	2.595	F(3) ... F(1 <sup>v</sup> )	3.157
F(2) ... F(4 <sup>iii</sup> )	2.985	P(2) ... F(4 <sup>iv</sup> )	3.170
F(4) ... F(3 <sup>iii</sup> )	3.003	F(3) ... F(1 <sup>iv</sup> )	3.174
F(2) ... F(3 <sup>iii</sup> )	3.008	F(1) ... F(2 <sup>iv</sup> )	3.222
F(1) ... H(1 <sup>iv</sup> )	3.096	N(1) ... F(3 <sup>iii</sup> )	3.229
F(1) ... F(1 <sup>iv</sup> )	3.105	P(2) ... F(2 <sup>vi</sup> )	3.232
F(3) ... F(4 <sup>iv</sup> )	3.109	N(1) ... F(1 <sup>iv</sup> )	3.298

(b) Important angles (°)

F(3)-P(2) ... F(4 <sup>iv</sup> )	73.3	N(1)-P(2) ... F(4 <sup>iv</sup> )	85.6
F(3)-P(2) ... F(2 <sup>vi</sup> )	67.6	N(1)-P(2) ... F(2 <sup>vi</sup> )	158.3
F(4)-P(2) ... F(4 <sup>iv</sup> )	168.8	N(1)-H(1) ... F(1 <sup>iv</sup> )	152
F(4)-P(2) ... F(2 <sup>vi</sup> )	66.8	N(1)-H(1) ... F(3 <sup>iii</sup> )	131
		F(1 <sup>iv</sup> ) ... H(1) ... F(3 <sup>iii</sup> )	76

(c) Closest approaches (Å) involving P(1)

P(1) ... F(4 <sup>iv</sup> )	3.539	F(4) ... P(1 <sup>viii</sup> )	3.781
P(1) ... F(1 <sup>iv</sup> )	3.726	P(2) ... P(1 <sup>viii</sup> )	3.804

Roman numerals as superscripts refer to the following equivalent positions relative to the reference molecule at  $x, y, z$ :

I	$1-x, 1-y, 1-z$	V	$1-x, -y, 1-z$
II	$\frac{1}{2}-x, \frac{1}{2}+y, \frac{1}{2}-z$	VI	$x-\frac{1}{2}, \frac{1}{2}-y, z-\frac{1}{2}$
III	$\frac{1}{2}+x, \frac{3}{2}-y, \frac{1}{2}+z$	VII	$x-\frac{1}{2}, \frac{3}{2}-y, z-\frac{1}{2}$
IV	$x, y-1, z$	VIII	$\frac{3}{2}-x, \frac{1}{2}+y, \frac{1}{2}-z$

and calculated structure factors and thermal parameters is available as Supplementary Publication No. SUP 22481 (5 pp.).\*

Bis(difluorophosphino)amine was prepared as described before,<sup>1</sup> and its purity checked spectroscopically. Infrared spectra were recorded using a Perkin-Elmer 225 double-beam spectrometer.

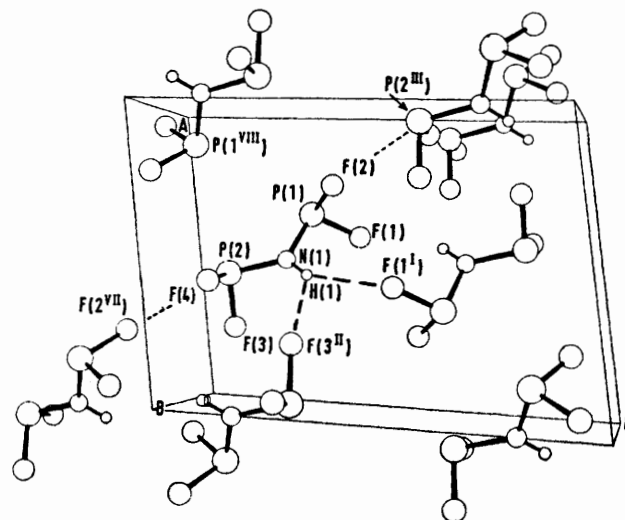


FIGURE 1 Arrangement of molecules in the unit cell; the atomic labelling scheme is indicated. Molecules separated by a unit translation along the  $b$  axis (as shown at top right) are 'connected' by  $P(2) \cdots F(4)$  interactions

Calculations were performed on computers of the Edinburgh Regional Computing Centre using programs written here together with the systems 'X-RAY '72'<sup>9</sup> and PLUTO.<sup>10</sup>

*Vibrational Spectra.*—The i.r. spectrum of gaseous  $NH(PF_2)_2$  has been reported before, but no information was given for the solid.<sup>1</sup> We have therefore recorded the i.r. spectra of solid samples in the regions associated with NH stretching (*ca.* 3400  $cm^{-1}$ ) and in plane NH deformation (*ca.* 1250  $cm^{-1}$ ). The spectrum of the vapour contains two bands of roughly equal intensity in each of these regions. The results are presented in Table 4. In the NH

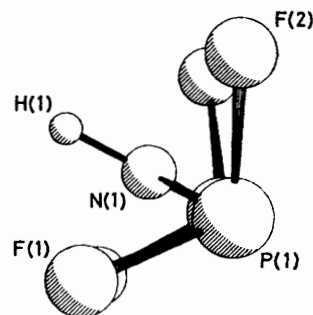


FIGURE 2 View of a single molecule showing the approximate  $C_{2v}$  symmetry. F(3) and F(4) are almost exactly eclipsed by F(1) and F(2). The 'torsion' angles  $F(1)-P(1) \cdots P(2)-F(3)$  and  $F(2)-P(1) \cdots P(2)-F(4)$  are  $-6.0$  and  $-6.8^\circ$  respectively

stretching region, only one band was observed in the spectrum of the solid, even when the spectrum was recorded within 20 s of spray-on. The frequency of this band corresponded closely to that of the band at lower frequency

\* For details see Notices to Authors No. 7, *J.C.S. Dalton*, 1978, Index issue.

TABLE 4  
Infrared bands of  $\text{NH}(\text{PF}_2)_2$  in the 3 300—3 500  
and 1 180—1 300  $\text{cm}^{-1}$  regions

Vapour	Solid at 90 K	Annealed solid at 90 K
3 376m	3 310ms	3 309s,sp
3 315ms		
1 245ms		1 220w,sp
1 210ms	1 218ms	1 215s,sp

m = Medium intensity, s = strong, sp = sharp, w = weak.

in this region in the spectrum of the vapour. Annealing the sample led to sharpening of this band but to no other changes in the spectrum in this region. In the region associated with NH deformation, one strong band at a frequency corresponding to that of the lower-frequency NH deformation mode in the spectrum of the vapour was

TABLE 5  
Bond lengths ( $\text{\AA}$ ) and bond angles ( $^\circ$ ) in some  $\text{PF}_2$ -substituted amines

Compound	Technique	Ref.	Bond		Angle	
			P-N	P-F	F-P-F	P-N-Q
$\text{PF}_2(\text{NH}_2)$	e.d. at 23 $^\circ\text{C}$	12	1.661(7)	1.581(3)	95.3(11)	119(2) <sup>a</sup>
$\text{NH}(\text{PF}_2)_2$	X-ray at -110 $^\circ\text{C}$	This work	1.667(10)	1.578(5)	95.7(4)	120.7(4) <sup>b</sup>
$\text{NMe}(\text{PF}_2)_2$	e.d. at -35 $^\circ\text{C}$	13	1.680(6)	1.583(2)	95.1(3)	116.1(8) <sup>b</sup>
$\text{PF}_2(\text{NMe}_2)$	X-ray at -110 $^\circ\text{C}$	11	1.628(5)	1.610(4)	91.5(3)	122 <sup>c</sup>
	e.d. at 23 $^\circ\text{C}$	12	1.684(8)	1.589(3)	99(3)	118.3(6) <sup>c</sup>
$\text{N}(\text{PF}_2)_3$	e.d. at 25 $^\circ\text{C}$	2	1.712(4)	1.574(2)	97.1(5)	120 <sup>b</sup>
$\text{PF}_2[\text{NH}(\text{SiH}_3)]$	e.d. at 60 $^\circ\text{C}$	3	1.657(7)	1.574(3)	100.8(12)	127.9(7) <sup>d</sup>

e.d. = Electron diffraction. <sup>a</sup> Q = H. <sup>b</sup> Q = P. <sup>c</sup> Q = C. <sup>d</sup> Q = Si.

observed in the spectrum of the solid recorded within 20 s of spray-on, together with a much weaker band at the position of the higher-frequency band observed in the spectrum of the vapour. After 60 s the weaker band to higher frequency had disappeared. On annealing, the strong band became much sharper, and a weak second band could be detected to slightly higher frequency. Since this second band was at a frequency very different from that of the second band in the spectrum of the vapour, and since only one band was observed in the NH stretching region in the spectrum of the solid, we ascribe the second band to a second-order mode.

#### DISCUSSION

The structure of several amino-derivatives containing  $\text{PF}_2$  groups have been studied in the gas phase by electron diffraction, but only the structure of  $\text{PF}_2(\text{NMe}_2)$  has been determined in the crystal by X-ray diffraction.<sup>11</sup> It is therefore interesting to note that the P-N and F-P bonded distances found for  $\text{PF}_2(\text{NH}_2)$ ,<sup>12</sup>  $\text{PF}_2(\text{NMe}_2)$ ,<sup>12</sup>  $\text{NMe}(\text{PF}_2)_2$ ,<sup>13</sup> and  $\text{N}(\text{PF}_2)_3$ <sup>2</sup> in the gas phase are close to those we report here for crystalline  $\text{NH}(\text{PF}_2)_2$  (see Table 5). Similarly, the P-N-P angle in crystalline  $\text{NH}(\text{PF}_2)_2$  is somewhat wider than in  $\text{NMe}(\text{PF}_2)_2$ , but rather narrower than P-N-Si in  $\text{PF}_2[\text{NH}(\text{SiH}_3)]$ ; in each molecule, the co-ordination round the N atom is at least roughly planar. Thus the gross features of the molecular geometry in crystalline  $\text{NH}(\text{PF}_2)_2$  are very much as expected by comparison with the gas-phase electron-diffraction studies. In crystalline  $\text{PF}_2(\text{NMe}_2)$  however the P-N bond is shorter, the P-F bond longer, and the F-P-F angle narrower than would be anticipated.

Only one conformer is present in the crystal. The hydrogen atom is not well located but appears to be coplanar with N(1), P(1), and P(2). The angles P(1)-N(1)-H(1) [112(5) $^\circ$ ] and P(2)-N(1)-H(1) [127(5) $^\circ$ ] are not equal but this distortion is not significant. Were the hydrogen atom to be symmetrically placed then all four fluorine atoms would be approximately equidistant from and *cis* to the H atom. The experimental intramolecular H...F distances (2.50—2.74  $\text{\AA}$ ) are not so short as to suggest that this conformer is determined by strong intramolecular interactions of this type; similarly, the shortest intermolecular H...F contacts (2.50  $\text{\AA}$ ) imply that intermolecular H...F interactions are real but weak. The intermolecular P...F contacts, of which the shortest are *ca.* 3.20  $\text{\AA}$ , are likely to be of

similar importance in determining the conformation taken up in the crystal. The relationship between the physical phase and the i.r. spectrum bears out these conclusions. In the spectra of the annealed solid we observe only one NH stretching and only one NH bending mode; the associated bands are sharp, and show none of the characteristic features associated with conventional hydrogen bonding. In the spectrum of the vapour, the presence of two bands in each region suggests that two conformers are present; since the frequencies of the bands in the spectrum of the solid correspond closely with those of the lower-frequency component in each region in the spectrum of the vapour, it seems reasonable to conclude that the conformer in the vapour that is responsible for the lower-frequency bands is at least very much like that present in the crystal. Furthermore, the association of lower-frequency NH stretching vibrations with conformers in which the N-H bond is *trans* to a lone pair on an adjacent atom has been made before for different types of molecule.<sup>14</sup> We have no evidence from which to deduce the geometry of the second conformer present in the vapour phase.

These conclusions may be compared with those we drew<sup>3</sup> from our study of  $\text{PF}_2[\text{NH}(\text{SiH}_3)]$ . The i.r. spectrum of that compound, too, showed two bands of roughly equal intensity in both NH stretching and NH deformation regions. The radial distribution curve led us to conclude that the less-abundant conformer had the two P-F bonds *gauche* to the N-H bond, as found for crystalline  $\text{NH}(\text{PF}_2)_2$ . The i.r. spectrum of an annealed crystalline sample of  $\text{PF}_2[\text{NH}(\text{SiH}_3)]$  showed only one band in both NH stretching and NH deform-

ation regions, and the frequency of each of these bands corresponded with the frequency of the lower of the two bands in each region present in the spectrum of the vapour. It now seems probable that the conformer present in crystalline  $\text{PF}_2[\text{NH}(\text{SiH}_3)]$ , as in crystalline  $\text{NH}(\text{PF}_2)_2$ , had the P-F bonds *gauche* to the N-H bond. It follows, of course, that the NH stretching and bending modes of this conformer give rise to substantially stronger i.r. bands than do those of the other.

*Crystal Packing.*—Each fluorine atom makes its own

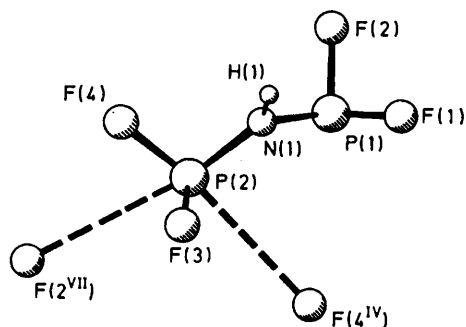


FIGURE 3 Arrangement of the three bonds and the two  $\text{P} \cdots \text{F}$  contacts around P(2)

contribution to the molecular packing through being involved in one, and only one, intermolecular interaction which is of type either  $\text{F} \cdots \text{P}$  or  $\text{F} \cdots \text{H}$ . The  $\text{P} \cdots \text{F}$  contacts (3.17 and 3.23 Å) are distinguished in that only one phosphorus atom, P(2), is involved. (The sum of van der Waals radii for P and F is  $1.8 + 1.5 \text{ \AA} = 3.3 \text{ \AA}$ .) In contrast, the shortest intermolecular contact to P(1) is at 3.54 Å. P(2) could be described as being pseudo-five-co-ordinated, having three short bonds and two long  $\text{P} \cdots \text{F}$  interactions (see Figure 3). Figure 1 shows how the sixth co-ordination position, that opposite to the P(2)–F(3) bond, is blocked by P(1<sup>VIII</sup>), where the  $\text{P}(2) \cdots \text{P}(1^{\text{VIII}})$  separation (3.80 Å) is 0.2 Å greater than the sum of van der Waals radii (3.6 Å). The  $\text{P} \cdots \text{F}$  interactions are presumably very weak and we find

no significant difference in the intramolecular P–N, P–F, N–P–F, or F–P–F parameters between the two ends of the molecule. The angles  $\text{N–P} \cdots \text{F}$  and  $\text{F–P} \cdots \text{F}$  (and also  $\text{N–H} \cdots \text{F}$ ), see Table 3(b), do however suggest an element of directional specificity. It seems that the  $\text{P} \cdots \text{F}$  and  $\text{F} \cdots \text{H}$  intermolecular contacts play an important role in determining the packing of molecules in the solid state, irrespective of their effect on the internal molecular conformation. We interpret the crystal packing in terms of molecules orientated to form infinite chains parallel to the *b* axis as a result of the  $\cdots \text{P}(2)\text{–F}(4) \cdots \text{P}(2)\text{–F}(4) \cdots$  interaction. Cross linking between adjacent chains is provided by the  $\text{P}(2) \cdots \text{F}(2)$  interactions and by the bifurcated  $\text{H}(1) \cdots \text{F}(1)$  and  $\text{H}(1) \cdots \text{F}(3)$  contacts.

We thank Mr. J. G. Wright for synthesising the sample used in the X-ray analysis.

[8/1532 Received, 21st August, 1978]

#### REFERENCES

- 1 D. E. J. Arnold and D. W. H. Rankin, *J.C.S. Dalton*, 1975, 889.
- 2 D. E. J. Arnold, D. W. H. Rankin, R. Seip, and M. R. Todd, *J.C.S. Dalton*, in the press.
- 3 D. E. J. Arnold, E. A. V. Ebsworth, H. F. Jessep, and D. W. H. Rankin, *J.C.S. Dalton*, 1972, 1681.
- 4 'International Tables for X-Ray Crystallography,' Kynoch Press, Birmingham, 1959, vol. 2, p. 299.
- 5 D. T. Cromer and J. B. Mann, *Acta Cryst.*, 1968, **A24**, 321.
- 6 R. F. Stewart, E. R. Davidson, and W. T. Simpson, *J. Chem. Phys.*, 1965, **42**, 3175.
- 7 'International Tables for X-Ray Crystallography,' Kynoch Press, Birmingham, 1974, vol. 4, p. 99.
- 8 Ref. 7, p. 149.
- 9 'X-RAY '72,' Technical Report TR-192, University of Maryland, 1972.
- 10 PLUTO, A program for Plotting Molecular and Crystal Structures, W. D. S. Motherwell, University Chemical Laboratory, Cambridge.
- 11 E. D. Morris and C. E. Nordman, *Inorg. Chem.*, 1969, **8**, 1673.
- 12 G. C. Holywell, D. W. H. Rankin, B. Beagley, and J. M. Freeman, *J. Chem. Soc. (A)*, 1971, 785.
- 13 E. Hedberg, L. Hedberg, and K. Hedberg, *J. Amer. Chem. Soc.*, 1974, **96**, 4417.
- 14 L. J. Bellamy and D. W. Mayo, *J. Chem. Phys.*, 1976, **80**, 1217.